Development/Plasticity/Repair

Inhibitory Plasticity Dictates the Sign of Plasticity at Excitatory Synapses

Lang Wang and Arianna Maffei
Department of Neurobiology and Behavior, State University of New York-Stony Brook, Stony Brook, New York 11794

The broad connectivity of inhibitory interneurons and the capacity of inhibitory synapses to be plastic make them ideal regulators of the level of excitability of many neurons simultaneously. Whether inhibitory synaptic plasticity may also contribute to the selective regulation of single neurons and local microcircuits activity has not been investigated. Here we demonstrate that in rat primary visual cortex inhibitory synaptic plasticity is connection specific and depends on the activation of postsynaptic $GABA_B$–Gi/o protein signaling. Through the activation of this intracellular signaling pathway, inhibitory plasticity can alter the state of a single postsynaptic neuron and directly affect the induction of plasticity at its glutamatergic inputs. This interaction is modulated by sensory experience. Our data demonstrate that in recurrent circuits, excitatory and inhibitory forms of synaptic plasticity are not integrated as independent events, but interact to cooperatively drive the activity-dependent rewiring of local microcircuits.

Key words: **excitatory synapses; GABA; inhibitory synapses; LTP; synaptic plasticity; visual cortex**

Introduction

Maturation of inhibitory synapses and development of a balance between excitation and inhibition mediate circuit refinement (Hensch and Fagiolini, 2005), sensory processing (Alitto and Dan, 2010), learning, and memory (Galindo-Leon et al., 2009). Inhibitory synaptic transmission can contribute to these processes through modulation of glutamatergic synaptic release (Pérez-Garci et al., 2013), modulation of the input/output function of a neuron (Saraga et al., 2008) or by compartmentalizing calcium signaling in postsynaptic neurons (Chiu et al., 2013). Inhibitory synapses are plastic (Nusser et al., 1998; Haas et al., 2006; Maffei et al., 2006; Nugent et al., 2007; Kurotani et al., 2008), their strength can be modulated by sensory experience (Maffei et al., 2006), and they contribute to experience-dependent circuit refinement (Yazaki-Sugiyama et al., 2009; Heimel et al., 2011), substance abuse (Madhavan et al., 2010), and chronic pain (Eto et al., 2012). Thus, inhibitory inputs may perform complex functions beyond general modulation of circuit excitability. Inhibitory synaptic plasticity is emerging as a fundamental regulator of circuit function; however, its mechanisms of induction and its role in neural circuits are poorly understood.

Here, we used the circuit in layer 4 (L4) of rat primary visual cortex (V1), in which a form of long-term potentiation of inhibitory synapses (LTPi) is inducible at fast spiking (FS) to pyramidal neurons synapses (Maffei et al., 2006), to investigate the mechanisms for LTPi and the effect of LTPi on recurrent excitatory inputs. We show that LTPi is connection-specific, depends on postsynaptic activity, and requires $GABA_B$ receptors activation. We also demonstrate that LTPi induction alters the capacity for plasticity at excitatory inputs. The crosstalk between excitatory and inhibitory plasticity is modulated by brief changes in visual drive.

Our findings have important implications for neural circuit function. The connection specificity of LTPi and its dependence on postsynaptic activity lead to potentiation of inhibitory synapses selectively onto pyramidal neurons that are active within a well identified range, allowing for precise refinement/rewiring of local microcircuits. The activation of the $GABA_B$–Gi/o protein signaling in the postsynaptic pyramidal neuron constrains the sign of synaptic plasticity inducible at converging recurrent glutamatergic inputs. Together, these mechanisms allow FS-mediated inhibition to regulate activity of pyramidal neurons with a high degree of specificity, despite their widespread connection probability. Although inhibitory and excitatory forms of plasticity are often debated as independent mechanisms, our data show that they are not independent events, but they cooperatively interact to shape cortical circuit connectivity and function.

Materials and Methods

All experimental procedures were approved by the Institutional Animal Care and Use Committee of Stony Brook University and followed the guidelines of the National Institutes of Health.

Visual deprivation. Monocular deprivation with eyelid suture (Maffei et al., 2004, 2006, 2010; Maffei and Turrigiano, 2008) was started at postnatal day 25 (P25) and maintained for 2–3 d. Briefly, animals were deeply anesthetized with a mixture of 70 mg/kg ketamine, 3.5 mg/kg xylazine hydrochloride, and 0.7 mg/kg acepromazine maleate injected intraperitoneally. The area around the eyelid was disinfected with beta-

Received Nov. 6, 2013; revised Dec. 4, 2013; accepted Dec. 6, 2013.

Author contributions: L.W. and A.M. designed research; L.W. and A.M. performed research; L.W. and A.M. analyzed data; L.W. and A.M. wrote the paper.

This work was supported by NIH Grant R01 EY019885 to AM. We thank Martha Stone, Michelle Kloc, Trevor Griffen, Melissa Haley, Dr. Alfredo Fontanini, Dr. Lorna Role, and Dr. Yury Garkun at State University of New York (SUNY)-Stony Brook for feedback on the paper, and Dr. Gina Turrigiano at Brandeis University for useful comments and discussions.

Correspondence should be addressed to Dr. Arianna Maffei, Department of Neurobiology and Behavior, Life Science Building, Room 548, SUNY-Stony Brook, Stony Brook, NY 11794. E-mail: Arianna.maffei@stonybrook.edu.

DOI:10.1523/JNEUROSCI.4711-13.2014

 0270-6474/14/341083-11$15.00/0

dine and 3–4 mattress sutures were placed using a 6-0 polyester sterile thread. At the end of the procedure, animals were allowed to recover on a heating pad and placed back in their cage only when fully alert. The sutured eye was checked every day to ensure full closure. Only animals whose sutures were perfectly preserved were used for recordings. The visual deprivation was done blind to the experimenter.

Brain slice preparation. P25–P28 Long–Evans rats of both sexes (Charles River) were anesthetized with isofluorane and decapitated. Acute coronal slices (300 μm) containing the monocular portion of V1 were prepared as previously described (Wang et al., 2012). Brain slices were incubated in standard artificial CSF (ACSF) at room temperature for at least 1 h before recordings. ACSF contained the following (in mM): 126 NaCl, 3 KCl, 25 $NaHCO_3$, 1 $NaHPO_4$, 2 $MgSO_4$, 2 $CaCl_2$, 14 Dextrose, pH 7.4 when bubbled with mixed 95% CO_2 and 5% O_2. A visual cortical slice was then transferred to the recording chamber and perfused with modified ACSF (in mM: 125 NaCl, 2.5 KCl, 25 $NaHCO_3$, 1.25 $NaHPO_4$, 1 $MgSO_4$, 2 $CaCl_2$, 25 dextrose) that allowed for easier detection of small monosynaptic responses. Recordings were performed at 32°C. The internal solution used in all of the experiments contained the following (in mM): 100 K-glutamate, 20 KCl, 10 K-HEPES, 4 Mg-ATP, 0.3 Na-GTP, 10 phosphocreatine, and 0.2% biocytin; pH was adjusted to 7.35 by KOH. In a subset of experiments the internal solution used to record from the postsynaptic neuron contained the following (in mM): 100 K-glutamate, 20 KCl, 10 K-HEPES, 4 Mg-ATP, 0.3 Na-GTP, 10 phosphocreatine, 5 BAPTA, and 0.2% biocytin; pH was adjusted to 7.35 by KOH. Osmolarity was adjusted to 295 mOsm with sucrose.

Electrophysiology. To record monosynaptic connections, quadruple whole-cell recordings were obtained from visually identified pyramidal neurons and FS in L4 of the monocular region of V1. Once the whole-cell configuration was established, depolarizing current pulses (700 ms) with 50 pA step increments were applied to elicit action potentials (APs). This allowed us to identify neuron subtypes based on firing properties. The identity and location of recorded neurons was further confirmed by *post hoc* morphology reconstruction. During recordings neuron resting membrane potential was maintained at −70 mV by injecting small DC currents. To assess the quality of the recordings, input resistance was monitored throughout the experiments. Neurons with >20% change in input resistance were not included in the analysis. To identify monosynaptic connections between recorded neurons, neurons were activated suprathreshold with 5 × 5 ms depolarizing pulses delivered at 20 Hz. These trains were staggered in time, and the unitary EPSP or IPSP was identified by computing the spike-triggered average of 30 traces recorded from putative postsynaptic neurons. Once the unitary EPSP or IPSP was detected, the baseline monosynaptic response was recorded for 10 min to assess stability and quantify the baseline properties of excitatory or inhibitory responses. After that, an induction paradigm was delivered to determine the plasticity of excitatory and/or inhibitory synapses. In experiments that required bath perfusion of a drug, an additional 10 min baseline was acquired before induction and the effect of the drug on baseline synaptic responses was quantified. To assess whether significant changes in synaptic strength were induced by the various induction paradigms, the EPSPs (or IPSPs) recorded 10 min before induction were compared with EPSPs (or IPSPs) recorded in the 30–40 min interval postinduction.

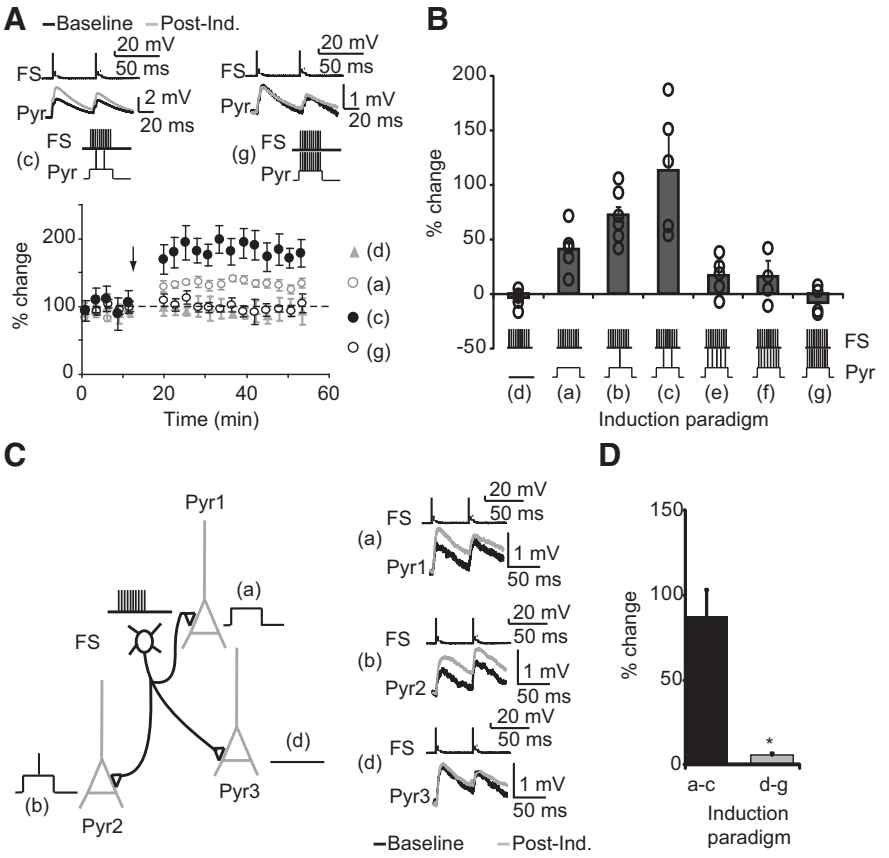

Figure 1. LTPi depends on postsynaptic activity and is connection-specific. ***A***, Top, Sample traces of monosynaptic IPSPs before (black) and after (gray) induction. Induction paradigms used in those experiments were 8 Hz (***Bc***, left) and 50 Hz (***Bg***, right). See ***B*** for further description of induction paradigms. ***A***, Bottom, Time course of percentage changes in IPSP amplitude induced with four different paradigms. ***B***, Bar plot of the magnitude of LTPi versus postsynaptic neurons activity for all pairs tested. Postsynaptic action potentials were elicited with 3 ms pulses delivered on top of a depolarizing step that was adjusted to achieve similar depolarization levels. Induction paradigms consist of 20 repetitions of the pairing shown at the bottom of each bar. The frequency of repetition was 0.1 Hz. ***C***, Left, Diagram of experimental configuration and sample traces of a FS neuron connected to three pyramidal neurons. Pairings ***Ba***, ***Bb***, and ***Bd*** were applied at the three different connections. ***C***, Right, Sample traces before (black) and after (gray) LTPi induction with the pairing shown in the diagram. Note the successful induction of LTPi only with pairings ***Ba*** and ***Bb*** onto Pyr 1 and Pyr 2. ***D***, Bar plot of average percentage changes in IPSP amplitude induced by pairings ***Ba***–***Bc***, black bar; and pairings ***Bd***–***Bg***, gray bar. Data from multiple triplets/quadruplets were pooled in the average bar plot. Right, Bar plot of the average change in IPSP amplitude in ***Ba***–***Bc*** (black; $n = 7$) and ***Bd***–***Bg*** pairings (gray; $n = 6$). Data are presented as mean ± SE. Asterisks indicate significant differences. To favor readability asterisks were not added to highlight significant differences in ***A***. The *p* values of one-way ANOVA and *post hoc t tests* are reported in Results.

Induction paradigms. To induce LTPi, 20 pairings of 10 FS action potentials at 50 Hz and postsynaptic depolarization of the pyramidal neuron were repeated at 0.1 Hz as previously reported (Maffei et al., 2006). To induce plasticity at recurrent excitatory synapses, trains of 10 presynaptic spikes at 50 Hz were evoked in the presynaptic pyramidal neuron and repeated 20 times at 0.1 Hz, while the membrane potential of postsynaptic pyramidal neuron was maintained at −70 mV (Wang et al., 2012). For testing the integration of excitatory and inhibitory plasticity, the protocols for inducing the plasticity of excitatory and inhibitory synapses were codelivered with a 2 s interval in recording configurations in which a FS neuron and a pyramidal neurons were both presynaptic to the same postsynaptic pyramidal cell (see Figs. 5*A*, 9*A*). The 2 s interval was chosen to allow complete recovery of the postsynaptic membrane from activation of possible intrinsic conductance in response to the depolarizing step required for LTPi or in response to bursts of APs elicited in the presynaptic pyramidal neuron. When isolating triplets for coinduction experiments, we ensured that FS was not directly activated by firing of either pyramidal neuron recorded simultaneously. Configurations in

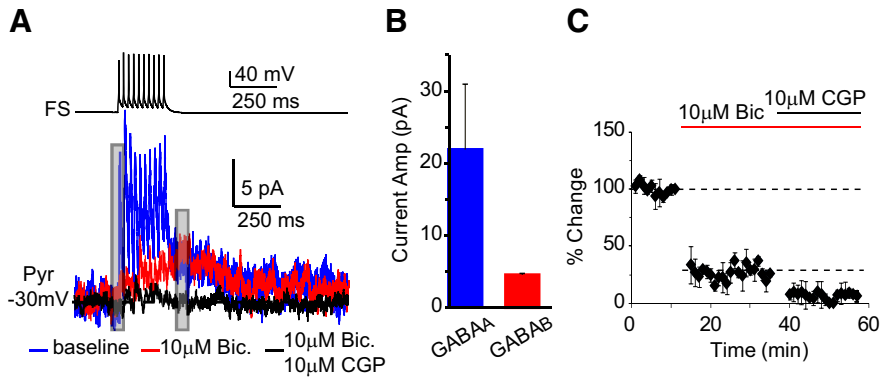

Figure 2. A single FS burst at 50 Hz evokes $GABA_A$- and $GABA_B$-receptor-activated currents. ***A***, Sample traces of FS neuron firing and postsynaptic $GABA_A$ (blue) and $GABA_B$ (red) currents. FS action potentials were elicited with 10–5 ms suprathreshold depolarizing steps delivered at 50 Hz. Bath application of bicuculline allowed the isolation of the $GABA_B$ current. Coapplication of bicuculline and CGP52432 abolished both $GABA_A$- and $GABA_B$-mediated currents (black). ***B***, Average amplitude of $GABA_A$ and $GABA_B$ receptor mediated currents. ***C***, Time course of changes in IPSP amplitude following bath perfusion of bicuculline and bicuculline + CGP52432. Gray bars on sample traces in ***A*** indicate the site of measurements of peak currents. Data are presented as mean ± SE.

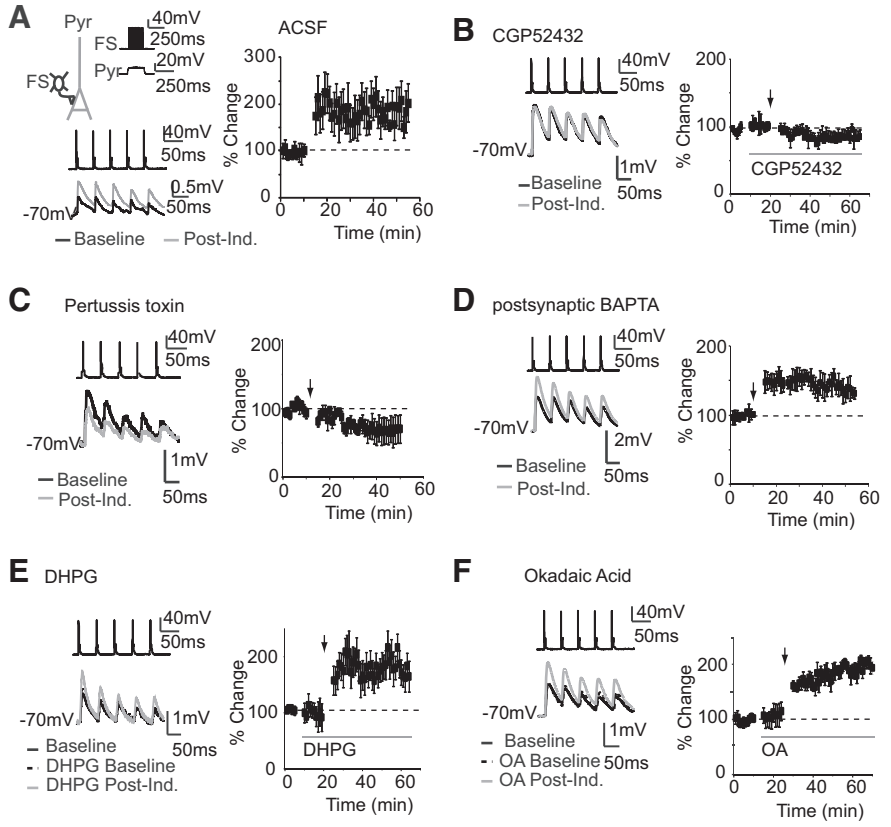

Figure 3. LTPi depends on $GABA_B$-Gi/o signaling. ***A***, Right, Diagram of experimental configuration and induction paradigm. Bottom left, Sample traces of LTPi induction in ACSF. Bottom right, Time course of LTPi in ACSF. ***B***, Example traces of IPSP in normal ACSF (black), in CGP52432 (dotted), after LTPi induction in CGP52432 (gray). Right, Time course of LTPi in CGP52432. Gray bar, Bath application of CGP52432. ***C***, Example traces of IPSP in PT recorded before (black) and after (gray) induction. Right, Time course of LTPi in PT. ***D***, Example traces of IPSP before (black) and after (gray) induction in the presence of postsynaptic BAPTA. Right, Time course of LTPi. ***E***, Example traces of IPSP in normal ACSF (black), following bath application of DHPG (dotted) and after LTPi induction in DHPG (gray). Right, Time course of LTPi in DHPG. Gray bar, Application of DHPG. ***F***, Example traces of IPSP in normal ACSF (black), in OA (dotted), and after LTPi induction in OA (gray). Right, Time course of LTPi in the presence of OA. Gray bar, Bath application of OA. Arrows indicate time of LTPi induction. Data are presented as mean ± SE.

which bidirectional connections were observed within the triplet were not included in the analysis.

Post hoc *neuronal reconstruction*. After recordings, slices were incubated in 4% paraformaldehyde in PBS for 1 week. After the incubation period, slices were washed with PBS, permeabilized in PBS containing 1% Triton X-100 for 2 h, and then incubated in streptavidine-AlexaFluor 488 (1:2000) dissolved in PBS containing 0.1% Triton X-100 at 4°C overnight. Slices were washed with PBS then mounted with fluoromount (Vector Laboratories). Stack images were collected using a confocal microscope (Leica) to allow for identification of neuronal morphology and location of the recordings. Only confirmed inhibitory and excitatory pairs within L4 were used for the analysis.

Data analysis. All data are expressed as mean ± SEM. Paired *t* test was used to determine the statistical significance of LTP and LTD within a condition. To compare the data across different conditions, the statistical significance is determined with one-way ANOVA and *post hoc* unpaired *t* test combined. Values of $p < 0.05$ are considered significant.

Results

We first identified the mechanisms of LTPi at FS to star pyramidal neuron synapses in L4 of V1. Then we asked whether the LTPi modulates the capacity for plasticity at recurrent glutamatergic synapses. Finally, we tested the effect of brief manipulation of visual drive on the interaction between excitatory and inhibitory synaptic plasticity. The first group of experiments required recordings of monosynaptic connections from a single FS onto multiple pyramidal neurons (Fig. 1*B*). The second and third set of experiments required the isolation of microcircuits with one FS and one pyramidal neuron presynaptic to the same pyramidal cell (see Figs. 5*A*, 9*A*). These recordings were obtained using multiple simultaneous patch-clamps between visually identified neurons in acute coronal slices from P25–P28. In a set of experiments visual deprivation was started at P25 and recordings were performed at P27–P28.

LTPi: parameter space and connection specificity

To understand the role of LTPi, we first needed to determine the parameter space for its induction. We asked whether success and magnitude of LTPi depend on postsynaptic activity. To test that, FS neurons were made to fire 20 bursts of action potentials at 0.1 Hz. Each burst contained 10 action potentials at 50 Hz (Maffei et al., 2006). In different recordings, FS bursting was paired with different patterns of star pyramidal neuron activity (Fig. 1*Aa–Ag*). We confirmed that when postsynaptic neurons were maintained at rest (Fig. 1*Ad*) LTPi was not induced, and when the postsynaptic neuron was depolarized from −70 mV to −55 mV (Fig. 1*Aa*), IPSP amplitude was potentiated [Fig. 1*Ad*, percentage change: −3.6 ±

5.3%; $n = 5$; $p = 0.5$; *Aa*, percentage change: 41.2 ± 5.6%; $n = 5$; within-pair paired *t* test (wp-p *t* test), $p < 0.01$]. The magnitude of LTPi increased if the postsynaptic neuron fired action potentials at low frequencies on top of the depolarizing step (Fig. 1*Ba–Bc*), with the largest increase for postsynaptic firing frequencies ~10 Hz (Fig. 1*Bc*; one-way ANOVA across *Ba–Bg*: $p < 0.05$; *Bb*, percentage change: 72.8 ± 7.1%; $n = 6$; wp-p *t* test, $p < 0.01$; *Bc*, percentage change: 133.1 ± 36.9%; $n = 5$; wp-p *t* test, $p < 0.01$; *post hoc t* test *Ba* vs *Bb*, *Ba* vs *Bc*), *Bb* vs *Bc*, $p < 0.05$). Increasing postsynaptic firing to 20 Hz (Fig. 1*Be*), 40 Hz (Fig. 1*Bf*), and 50 Hz (Fig. 1*Bg*) did not change IPSP amplitude (Fig. 1*Be*, percentage change: 16.7 ± 13.1%; $n = 5$; wp-p *t* test, $p = 0.4$; *Bf*, percentage change: 15.9 ± 15.2%; $n = 4$; wp-p *t* test, $p = 0.6$; *Bg*, percentage change: −8.2 ± 1.5%; $n = 5$; wp-p *t* test, $p = 0.3$; *post hoc t* tests, *Ba*, *Bb*, *Bc* vs *Bd*, *Be*, *Bf*, *Bg*, $p < 0.05$; *post hoc t* test, *Bd*, *Be*, *Bf*, *Bg* against one another, $p > 0.4$). Our data demonstrate that changes in IPSP amplitude are induced only when FS bursting is paired with pyramidal neurons active subthreshold (Fig. 1*Ba*) or in the low-to-medium frequency range (Fig. 1*Bb*,*Bc*).

FS contact many star pyramidal neurons. If repetitive bursting of one FS leads to LTPi at all its inhibitory inputs, a single FS would simultaneously affect the excitability of a large portion of L4. Alternatively, LTPi may be induced only at FS synapses onto pyramidal neurons that are active in the subthreshold to 10 Hz range (Fig. 1*Ba–Bc*), conferring this form of plasticity connection specificity despite high connection probability. To assess this, we performed multiple simultaneous patch-clamp recordings to isolate connections from a single FS onto 2–3 star pyramidal neurons (Fig. 1*C*). Once the appropriate configuration and a stable baseline were obtained, FS bursting was paired with different patterns of postsynaptic activity *a–g* at each connection (Fig. 1*C*). In simultaneously recorded connections only *a–c* pairings produced LTPi, whereas pairings *d–g* left IPSPs unchanged. On average paradigms *a–c* produced 86.9 ± 16.8% potentiation, whereas *d–g* showed 5.6 ± 1.1% change in IPSP amplitude (Fig. 1*D*, a–c: $n = 7$ pairs; d–g: $n = 6$; *t* test between groups *Ba–Bc* and *Bd–Bg*: $p < 0.002$). Together, these data indicate that LTPi is connection-specific despite widespread FS connectivity.

Mechanisms of LTPi

The mechanisms of LTPi are unknown. FS bursting releases GABA that could activate $GABA_A$ and $GABA_B$ receptors (Gonchar et al., 2001). We tested the hypothesis that LTPi may be a $GABA_B$-dependent potentiation of $GABA_A$ IPSPs. First we asked whether a 10-spike FS burst at 50 Hz like that used for LTPi could elicit $GABA_B$-IPSCs in the postsynaptic neuron (recorded in voltage-clamp at −30 ± 5 mV, ~20 mV above the reversal potential for chloride set by our internal solution; −49.7 mV). Monosynaptic IPSCs were composed of a $GABA_A$-mediated current, sensitive to 20 μM bicuculline, and a slow, $GABA_B$-mediated component blocked by 10 μM CGP52432 (Fig. 2; $GABA_B$ IPSC: 4.25 ± 0.2 pA, $n = 5$). Thus, bursting of a single FS engages $GABA_A$ and $GABA_B$ signaling in L4 pyramidal neurons.

We verified that LTPi is reliably induced in our experimental conditions [Fig. 3*A*; ACSF, percentage change IPSP: 66.8 ± 21.5%; $n = 8$; paired *t* test (p *t* test), $p < 0.01$]. The dependence of LTPi on $GABA_B$ was then tested. Once a FS-pyramidal neuron connection was identified and a 5 min baseline acquired, CGP52432 (10 μM) was bath applied and IPSPs were monitored for 10 min to control for direct effects of CGP52432. IPSPs were monitored for at least 40 min after induction paradigm. LTPi was quantified by comparing IPSPs amplitude in the 10 min baseline-CGP52432 perfusion with that of IPSPs recorded in the 30–40 min postinduction interval. $GABA_B$ blockade did not affect baseline IPSPs, but impaired LTPi (Fig. 3*B*; CGP, percentage change-baseline: 15.2 ± 11.8%; $p = 0.6$; percentage change-LTPi: −18.5 ± 8.4%; $n = 11$; p *t* test, $p = 0.8$). The same effect was observed with 1 μM CGP52432 (1 μM CGP, percentage change-LTPi: 2.8 ± 6.4%; $n = 10$; p *t* test, $p = 0.8$). These data demonstrate that LTPi requires $GABA_B$ receptors activation.

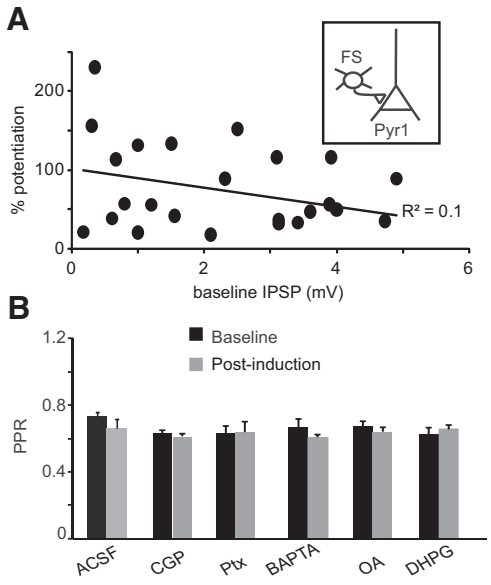

Figure 4. LTPi is independent on the baseline IPSP amplitude and does not affect paired pulse ratio. ***A***, Plot of the magnitude of LTPi versus baseline IPSP amplitude for each pair tested. Note that there was no significant correlation. ***B***, In all LTPi induction groups there were no significant changes in PPR before (black) and after (gray) induction, suggesting that LTPi has a postsynaptic site of expression.

$GABA_B$ receptor signaling depends on Gi/o proteins. Incubation of slices treated with pertussis toxin (PT; 0.2 μg/ml) for 4–6 h before recording, a treatment preventing dissociation of α and $\beta\gamma$ subunits of the Gi/o protein, was used to assess the involvement of Gi/o proteins in LTPi. PT was maintained in the bath throughout the experiment. PT prevented LTPi (Fig. 3*C*; percentage change-IPSP: −22.6 ± 9.3%; $n = 6$; p *t* test, $p = 0.1$). This effect did not depend on slices age as LTPi is routinely induced after maintaining them in oxygenated ACSF for >6 h. Our data demonstrate that LTPi is a $GABA_B$-dependent potentiation of $GABA_A$ IPSPs mediated by Gi/o signaling.

In layers 2/3 and 5 of V1, inhibitory synaptic potentiation is calcium-dependent (Komatsu, 1996; Holmgren and Zilberter, 2001). We thus asked whether LTPi in L4 might also require calcium signaling. When BAPTA (5 mM) was selectively added to the postsynaptic pyramidal neuron, LTPi was not affected (Fig. 3*D*; BAPTA, percentage change-IPSP: 50.4 ± 10.6%; $n = 7$; p *t* test, $p < 0.01$). Group I metabotropic glutamate receptors (mGluR) may play a role in plasticity of inhibitory synapses (Sugiyama et al., 2008). Although in our experiments we used paired recordings of FS and star pyramidal neurons, tonic levels of glutamate could activate mGluRs. To assess whether Group I mGluRs facilitate LTPi, we applied their selective agonist 50 μM DHPG. DHPG did not affect baseline IPSPs, LTPi induction, and magnitude (Fig. 3*E*; DHPG, percentage change-baseline: 4.9 ± 14.9; p *t* test, $p = 0.5$; percentage change- LTPi: 74.1 ± 23.2%; $n = 10$; p *t* test, $p < 0.01$). Gi/o protein signaling can impair adenyl cyclase and decrease protein kinase activity, possibly favoring signaling from protein phosphatases. Phosphatases were proposed

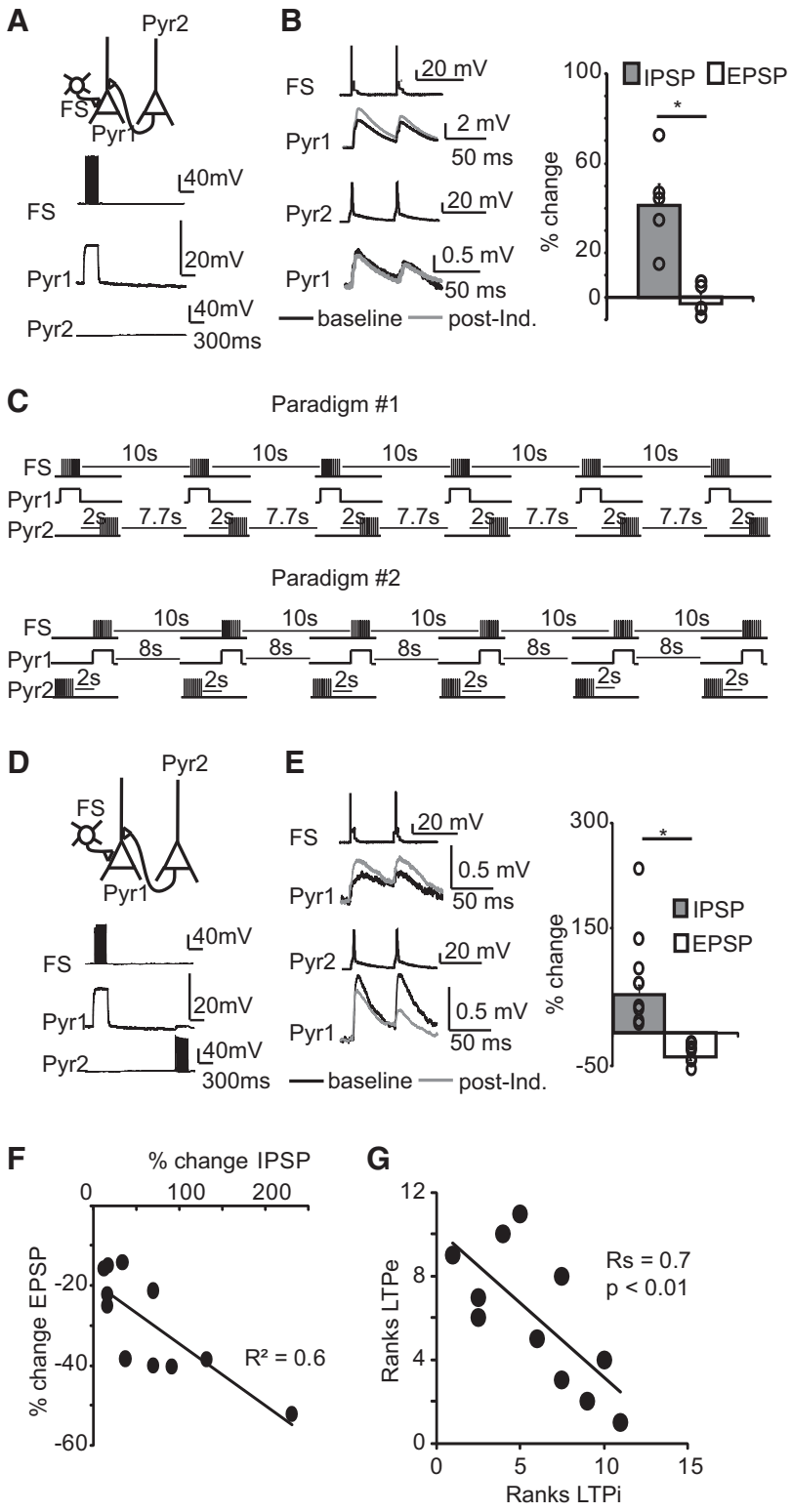

Figure 5. LTPi affects the sign of plasticity at recurrent excitatory synapses. ***A***, Top, Diagram of experimental configuration. Bottom, Raw traces during coinduction. ***B***, LTPi induction alone did not affect the amplitude of the converging monosynaptic EPSP. Top, Example traces of IPSPs. Black, baseline; gray, after LTPi induction. Bottom, Example traces of EPSPs before (black) and after (gray) LTPi induction. Right, Bar plot of percentage changes in IPSP and EPSP amplitude following LTPi induction. Open circles indicate IPSPs and EPSPs from single triplets. ***C***, Diagram of coinduction paradigms used for these experiments. ***D***, Top, Diagram of experimental configuration. Bottom, Raw traces of coinduction of LTPi and LTPe at converging inputs. ***E***, Top, Example traces of IPSPs. Black, baseline; gray, after coinduction. Bottom, Sample EPSPs before (black) and after (gray) coinduction. Right, Cumulative bar plot of percentage changes in IPSP and EPSP amplitude after coinduction of LTPi and LTPe. Open circles indicate IPSPs and EPSPs from single triplets. ***F***, Correlation of percentage changes in IPSP and EPSP amplitude after coinduction of LTPi and LTPe. ***G***, Spearman rank order correlation analysis of the magnitude of LTPe and LTDe. Data are presented as mean ± SE. Asterisks indicate significant differences.

as a downstream regulators of $GABA_B$ signaling (Chung et al., 2009), of $GABA_A$ receptors phosphorylation (Mansuy and Shenolikar, 2006), and mechanisms for synaptic plasticity (Belmeguenai and Hansel, 2005; Mansuy and Shenolikar, 2006). Blockade of protein phosphatases by 0.1 or 1 μM okadaic acid (OA) did not affect baseline IPSPs (Fig. 3*F*; percentage change-IPSP: 9.7 ± 14.7; $n = 8$; p *t* test, $p = 0.5$). LTPi was not prevented by either 0.1 or 1 μM OA (Fig. 3*F*; percentage change-OA: 40.8 ± 10.4%; $n = 8$, p *t* test, $p < 0.01$). Thus, L4 LTPi is independent of postsynaptic calcium, mGluR, and protein phosphatase signaling.

We asked whether baseline IPSP amplitude influences induction and/or magnitude of LTPi. There was no correlation between baseline IPSP amplitude and magnitude of successful LTPi (Fig. 4*A*; $R^2 = 0.1$; $n = 18$). Last, we quantified possible changes paired pulse ratio (PPR) following induction in all experimental conditions. LTPi left PPR unchanged (Fig. 4*B*; percentage change-PPR, LTPi: −8.6 ± 8.1%, $n = 8$, $p = 0.3$; CPG: −0.7 ± 3.1%, $n = 11$, p *t* test, $p = 0.6$; PT: 0.5 ± 4.6%, $n = 6$, $p = 0.7$; BAPTA: −7.7 ± 5.1%, $n = 5$, $p = 0.2$; OA: −1.5 ± 4.2%, $n = 7$, $p = 0.5$; DHPG: 6.6 ± 4.6%, $n = 8$, $p = 0.3$). These data support the interpretation that LTPi is expressed postsynaptically, and that the initial strength of the connection is not predictive of the sign of plasticity.

What is the role of LTPi?

How LTPi may affect neural circuits is unknown. In recurrent circuits such as neocortex, excitatory and inhibitory inputs converge onto a postsynaptic neuron, which needs to integrate them and produce the appropriate output. Overlap of the location of GABA and glutamate synapses was shown in the hippocampus (Pettit and Augustine, 2000) and in V1 (Chen et al., 2012). Interdependence of GABA and glutamatergic transmission has been recently reported in the hippocampus (Hayama et al., 2013), in neocortex (Chiu et al., 2013), and in the cerebellum (Hirono et al., 2001), suggesting local crosstalk between excitatory and inhibitory inputs. It is currently unknown how long term changes in excitatory and inhibitory synaptic strength may be integrated. We addressed this question directly, using multiple patch-clamp recordings to isolate microcircuits in which one FS and one pyramidal neuron (Pyr2) were presynaptic to the same pyramidal cell (Pyr1; Fig. 5*A*). In these experiments neither Pyr1, nor Pyr2 were presynaptic to FS or bidirectionally connected.

In the first set of experiments, we asked whether LTPi at FS-Pyr1 affects baseline EPSP amplitude of Pyr2-Pyr1. As shown in Figure 5*B*, LTPi did not affect Pyr2-Pyr1 EPSP amplitude, indicating that LTPi induction alone does not modulate recurrent EPSPs (Fig. 5*B*; FS-Pyr1-percentage change, 42.7 ± 16.3; $n = 4$; wp-p t test, $p < 0.01$; Pyr2-Pyr1-percentage change, −2.1 ± 3.1%; $n = 4$; wp-p t test, $p = 0.5$; percentage change IPSP vs percentage change EPSP, unpaired t test, u t test, $p < 0.001$).

L4 recurrent synapses between pyramidal neurons are plastic, and after the onset of the critical period can undergo LTP (LTPe; Wang et al., 2012). We used the paradigm for LTPe to investigate how LTPe and LTPi may be integrated by the postsynaptic neuron. Paradigms for LTPi (Fig. 1*Ba*) and LTPe induction were coapplied at FS-Pyr1 and Pyr2-Pyr1 (Fig. 5*C*,*D*). A 2 s interval between FS and Pyr2 bursting was used to allow for complete relaxation of membrane charges due to Pyr1 postsynaptic depolarization (Fig. 5*C*, Paradigm #1). In this configuration, LTPi was induced, whereas LTPe was impaired. LTDe was induced instead (Fig. 5*D*,*E*; percentage change-IPSP-FS-Pyr1: 54.2 ± 13.7%, wp-p t test, $p < 0.01$; percentage change-EPSP-Pyr2-Pyr1: −34.4 ± 4.6%, wp-p t test, $p < 0.01$; percentage change-IPSP vs percentage change-EPSP, u-t test: $p < 10^{-4}$; $n = 11$). These results suggest that LTPi and LTPe are not integrated as independent events.

The interaction could be specific to the order of pairing. To assess that, we compared experiments in which FS-Pyr1 pairing preceded (Fig. 5*C*, Paradigm #1; $n = 5$) or followed Pyr 2 bursting (Fig. 5*C*, Paradigm #2; $n = 6$). There was a dominant effect of LTPi, which was always successful, whereas the input from Pyr2 showed only LTDe. Thus, data obtained in coinduction experiments were pooled in Figure 5. Successful LTPi and LTPe rely on 20 repetitions of the induction paradigms. Paradigm #2 (Fig. 5*C*) is therefore equal to a paradigm in which Pyr2 bursting follows FS-Pyr1 pairing by 8 s. This suggests that the interaction between LTPi and LTPe can occur over a time scale of few seconds. To further analyze the relationship between LTPi and plasticity at excitatory inputs, we asked whether the magnitude of changes in IPSP and EPSP amplitude were correlated. There was a significant correlation of the magnitude of LTPi and LTDe (Fig. 5*F*; $R^2 = 0.63$), further confirmed by Spearman rank order correlation analysis (Fig. 5*G*; $Rs = 0.7$, $p < 0.01$). Thus, LTPi directly affects the capacity for plasticity at converging glutamatergic synapses.

Mechanisms of crosstalk between inhibitory and excitatory plasticity

Crosstalk between excitatory and inhibitory plasticity was reported in several brain regions. This interaction can occur via modulation of chloride reversal potential (Ormond and Woodin, 2009), heterosynaptic retrograde signals (Chevaleyre and Castillo, 2003), or spillover of neurotransmitters onto presynaptic terminals (Nugent et al., 2009). What mediates the crosstalk between LTPi and excitatory plasticity in L4?

To assess whether heterosynaptic activation of presynaptic $GABA_B$ receptors mimics the effect of LTPi on LTPe, we pharmacologically activated $GABA_B$ receptors with baclofen (20 μM, bath applied). Baclofen decreased EPSP amplitude and increased PPR (Fig. 6*A*,*B*; percentage change-EPSP: −75.6 ± 5.2%; $n = 4$; p t test, $p < 0.01$; percentage change-PPR: 156.1 ± 49.2%; $n = 4$; p t test, $p < 0.01$). Baclofen often decreased EPSP amplitude below detection threshold (0.2 mV).

This effect is consistent with $GABA_B$-dependent reduction in release probability. These data demonstrate that in addition to being on postsynaptic terminals opposite FS, $GABA_B$ receptors are present at presynaptic glutamatergic synapses. However, baclofen did not mimic the effect LTPi on excitatory inputs (Fig. 5*B*): pharmacological activation of $GABA_B$ receptors decreases EPSP amplitude and increases PPR, whereas LTPi induction affects the capacity for plasticity of glutamatergic inputs without affecting baseline EPSP amplitude and PPR.

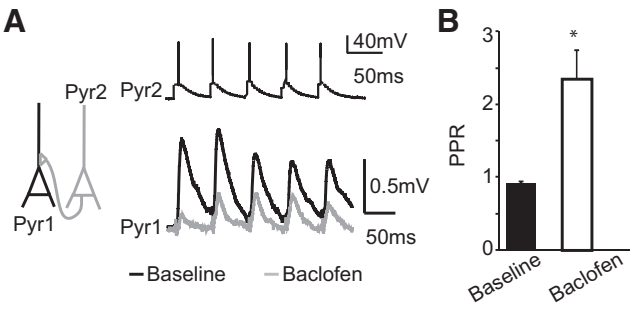

Figure 6. Baclofen reduces baseline EPSP amplitude. ***A***, Left, Diagram of recording configuration. Right, Sample paired recording between recurrently connected pyramidal neurons in layer 4. Black, EPSP before; gray, EPSP after bath application of baclofen. ***B***, Baclofen significantly increases the paired pulse ratio of recurrent EPSPs, further confirming that the effect of baclofen on baseline excitatory transmission is largely mediated by $GABA_B$ receptors located presynaptically.

FS elicit $GABA_B$-mediated IPSCs in L4 star pyramids (Fig. 2), suggesting that the crosstalk between LTPi and LTPe is likely to occur within postsynaptic neurons. To begin to unravel the mechanisms of crosstalk we asked whether interfering with $GABA_B$ signaling affects LTPe. We verified that LTPe is successfully induced in control conditions (Fig. 7*B*; ACSF percentage change-EPSPs: 33.8 ± 8.3; $n = 10$; p t test, $p < 0.05$). Then we observed that 1 μM CGP52432 did not prevent LTPe (percentage change-EPSP: 25.2 ± 8.4, $n = 11$; p t test, $p < 0.01$, data not shown). Preventing dissociation of α and $\beta\gamma$ subunits of the Gi/o protein with PT did not impair LTPe (Fig. 7*C*; percentage change-EPSP: 39.1 ± 14.4; $n = 5$; p t test, $p = 0.04$). PPR was significantly reduced following LTPe induction in PT, confirming that this form of plasticity is similar to the one induced in ACSF (Wang et al., 2012; Fig. 8*A*; LTPe percentage change-PPR: −24 ± 5.8, $n = 10$, $p < 0.01$; PT percentage change-PPR: −17.6 ± 2.7%, $n = 5$, p t test: $p < 0.04$). Thus, blocking $GABA_B$–Gi/o signaling does not affect baseline EPSPs, nor does it impair LTPe. LTPe magnitude did not correlate baseline EPSPs amplitude (Fig. 8*B*; $R^2 = 0.15$; Wang et al., 2012), indicating that LTPe is independent of the previous history of the synapse.

Gi/o signaling activates a number of cellular mechanisms that could interfere with LTPe. Gi/o activation reduces calcium entry through voltage-gated calcium channels (VGCC; (Pérez-Garci et al., 2013), prevents backpropagation of action potentials (Pérez-Garci et al., 2013), and can lead to the activation of mGluRs (Hirono et al., 2001). LTPe is induced even when the postsynaptic neuron is hyperpolarized (Wang et al., 2012), suggesting that postsynaptic NMDA receptors are not required. However, adding 5 mM BAPTA only in the postsynaptic neuron prevented LTPe (Fig. 7*D*; percentage change: 3.4 ± 15.9%; $n = 4$; p t test, $p = 0.9$), and the reduction in PPR associated with it (Fig. 8*A*; BAPTA percentage change-PPR: −7.4 ± 4.1%, $n = 5$, p t test, $p = 0.2$). L-type VGCC may be the source of calcium required for LTPe and a possible site of action of Gi/o signaling. Bath perfusion of 10 μM nifedipine blocked LTPe, inducing a significant LTDe (Fig. 7*E*; Nifedipine-percentage change: −30.8 ± 4.2, $n = 14$, p t test, $p < 0.01$). Postsynaptic BAPTA prevented LTPe but

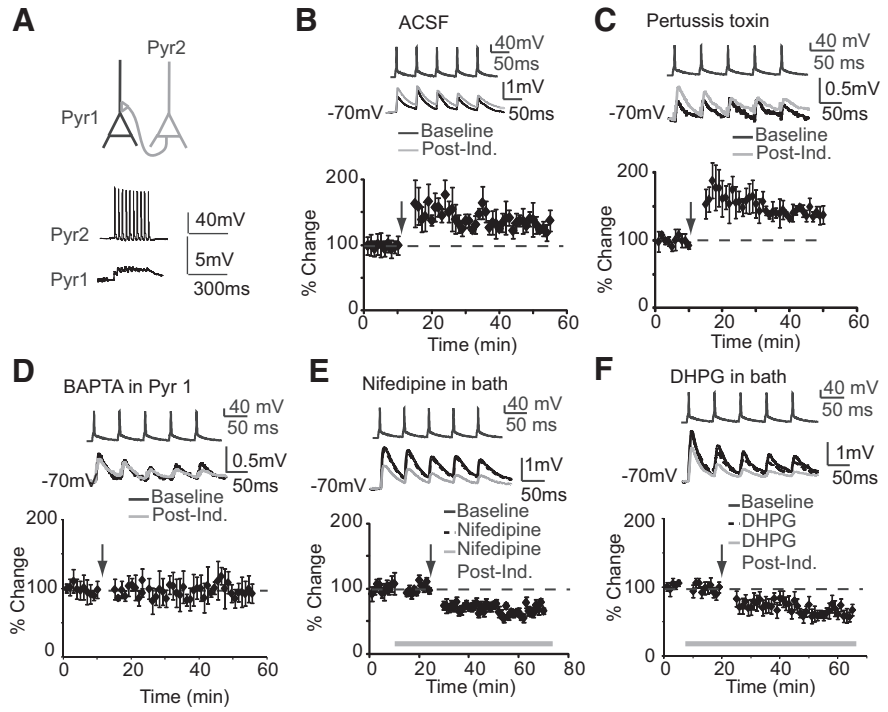

Figure 7. Mechanisms for LTPe. ***A***, Top, Diagram of recording configuration. Bottom, Raw traces of Pyr1 and Pyr2 during induction. ***B***, Top, Sample traces of EPSPs recorded before (black) and after (gray) LTPe induction in ACSF. Bottom, Time course of LTPe in ACSF. ***C***, Top, Sample traces before (black) and after (gray) LTPe induction in the presence of PT. Bottom, Time course of LTPe in PT. ***D***, Top, Sample traces before (black) and after (gray) LTPe induction in the presence of postsynaptic BAPTA. Bottom, Time course of LTPe in the presence of postsynaptic BAPTA. ***E***, Top, Sample traces of EPSPs recorded in regular ACSF (black), nifedipine (dotted), and after LTPe induction in nifedipine (gray). Bottom, Time course of LTPe in nifedipine. Gray bar, nifedipine application. ***F***, Top, Sample EPSPs in normal ACSF (black), in DHPG (dotted), and after LTPe induction in DHPG (gray). Bottom, Time course of LTPe in DHPG. Gray bar, bath application of DHPG. Data are mean ± SE.

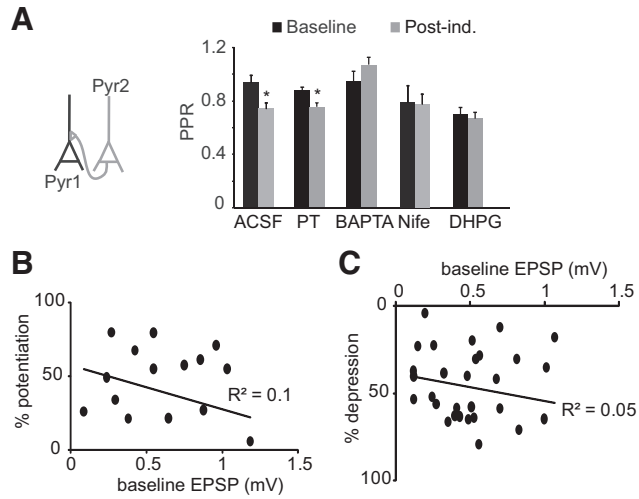

Figure 8. LTPe and LTDe differ in their site of expression, but the magnitude of both forms of plasticity is independent of baseline EPSP amplitude. ***A***, Left, Diagram of recording configuration. Right: there was a significant reduction in PPR only after successful LTPe induction. Pharmacological manipulations that impaired LTPe also impaired the change in PPR. When LTDe was induced, no changes in PPR were observed. ***B***, ***C***, Plots of the magnitude of plasticity versus the initial EPSP amplitude. Note that there was no significant correlation between these parameters both in the group in which LTPe was induced (***B***) and in the LTDe group (***C***).

did not lead to LTDe; differently blockade of L-type VGCC led to a significant depression, suggesting that L-type VGCC may affect LTPe by acting both on neuronal excitability and intracellular signaling.

LTD at glutamatergic synapses can also be facilitated by $GABA_B$-dependent activation of mGluRs. Activating Group I mGluRs with 50 μM DHPG did not affect baseline EPSPs, but impaired LTPe favoring LTDe (Fig. 7*F*; percentage change-baseline EPSP: 0.5 ± 4.5%; $n = 12$; $p = 0.6$; percentage change-EPSP after induction: −33.9 ± 5.4%; $n = 12$; p *t* test: $p < 0.01$). DHPG prevented the reduction in PPR associated with LTPe (Fig. 8*A*; DHPG percentage change-PPR: −7.6 ± 5.3%, $n = 12$, p *t* test, $p = 0.12$). In all conditions in which LTDe was induced, the magnitude of depression was independent of EPSP's initial amplitude (Fig. 8*C*; $R^2 = 0.05$; $n = 21$; Spearman rank order correlation coefficient, $Rs = -0.2$; two-tailed $p = 0.4$). Data were plotted together only after verification that correlations were not present within each group.

These data suggest multiple mechanisms for Gi/o signaling to mediate the crosstalk between LTPi and LTPe. We therefore tested whether pharmacological manipulation of Gi/o signaling could affect the outcome of coinductions. Once the recording configuration for coinduction was selected (Figs. 5*A*, 9*A*) LTPi and LTPe induction paradigms were coapplied as described above. Blockade of Gi/o signaling with PT prevented LTPi induction (Fig. 9*B*,*C*; percentage change-IPSP: −15.2 ± 10.9, $n = 12$ triplets; p *t* test: $p = 0.4$) while allowing for successful LTPe (LTPe: percentage change-EPSP: 33.6 ± 10.4, $n = 12$ triplets; p *t* test, $p < 0.01$; percentage LTPi vs percentage LTPe, *t* test, $p < 10^{-4}$). PT also disrupted the correlation between changes in EPSPs and IPSPs (Fig. 9*D*,*E*; R^2-PT = 0.04; Spearman rank order correlation: Rs − PT = 0.02, $p = 0.9$). These data support the interpretation that $GABA_B$–Gi/o signaling is not only needed for LTPi, but is also a determinant for the crosstalk between LTPe and LTPi.

Experience-dependent regulation of the crosstalk

LTPi and LTPe are both induced in the critical period for visual cortical plasticity (Maffei et al., 2006; Wang et al., 2012). Brief visual deprivation by unilateral eyelid suture saturates LTPi (Maffei et al., 2006) and changes the capacity for plasticity at L4 recurrent synapses(Wang et al., 2012). We asked whether manipulating visual drive could alter the crosstalk between LTPi and LTPe. Animals received unilateral eyelid suture at P25 and acute slices were prepared from the hemispheres ipsilateral (control) and contralateral (deprived) to the closed eye at P27–P28. Recordings were obtained from the monocular portion of V1 to allow for within animal comparison of control and deprived conditions. In the control hemisphere LTPi induction modulated the capacity for plasticity at convergent excitatory inputs as expected (Fig. 10*A*,*B*). LTPi was effectively induced, while the converging excitatory synapse underwent LTDe (Fig. 10*A*,*B*; LTPi: 33.5 ± 8.4%; LTDe: −26.6 ± 5.6%; wp-p *t* test, $p < 10^{-5}$; $n = 9$). The magnitude of LTPi correlated with the magnitude of LTDe, as confirmed with Spearman rank order correlation analysis (Fig. 10*C*,*D*; $R^2 = 0.7$; $Rs = 0.5$; $p < 0.05$). Thus, data from the control

hemisphere recapitulate the results obtained from nondeprived rats.

In slices from the deprived hemisphere, the average amplitude of FS to pyramidal neurons synapses was significantly larger than that in control (control: 0.7 ± 0.2 mV, $n = 8$; deprived: 3.1 ± 0.8 mV, $n = 7$; $p < 0.05$) as previously shown (Maffei et al., 2006). Further induction of LTPi resulted in depotentiation of IPSPs. Depotentiation alone did not affect baseline EPSP amplitude (Fig. 11; deprived, LTDi: −34.9 ± 20.6%, $p < 0.05$; LTPe: −0.6 ± 4.8%, p *t* test, $p = 0.81$, $n = 4$). However acute depotentiation of FS-mediated IPSP allowed for the recovery of LTPe at the input from Pyr2 (Fig. 10*E*,*F*; percentage change IPSP: −37.6 ± 6.3%; percentage change-EPSP: 70.3 ± 8.9%; p *t* test: $p < 10^{-6}$; $n = 6$). The magnitude of depotentiation correlated with that of LTPe (Fig. 10*G*; $R^2 = 0.8$), as further confirmed by Spearman rank order correlation analysis (Fig. 10*H*; $Rs = 0.9$; $p < 0.05$). These results support the interpretation that the capacity for excitatory and inhibitory plasticity and their integration are modulated by visual experience.

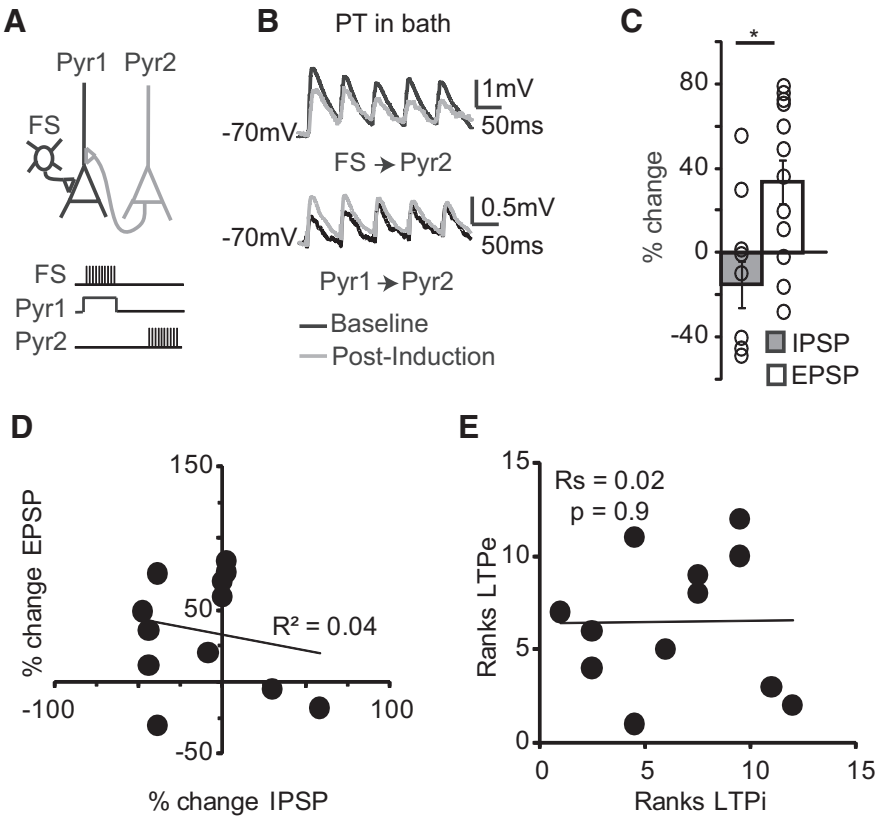

Figure 9. PT prevents LTPi and restores LTPe during coinduction. ***A***, Top, Diagram of experimental configuration. Bottom, Diagram of coinduction paradigms. ***B***, Sample traces of IPSPs (top) and EPSPs (bottom) recorded before (black) and after coinduction (gray) in the presence of PT. ***C***, Bar plot of percentage changes in IPSP and EPSP amplitude after LTPi and LTPe coinduction in PT. Open circles indicate single triplets. ***D***, Plot of percentage changes in EPSP amplitude versus percentage changes in IPSP amplitude following coinduction of LTPi and LTPe in PT. ***E***, Spearman rank order correlation of the magnitude of LTPe versus that of LTPi in the presence of PT. Data are mean ± SE. Asterisks indicate significant differences.

Discussion

We have shown that LTPi is connection specific and depends on postsynaptic activity, $GABA_B$ receptors, and Gi/o protein signaling. We have also demonstrated that acute changes in inhibitory synaptic strength affect the capacity for plasticity at excitatory inputs converging onto the same postsynaptic neuron. Our data support the interpretation that this interaction is mediated by crosstalk of signaling pathways activated by $GABA_B$, VGCC, and group I mGlu receptors (Fig. 12). Furthermore, the crosstalk we report is sensitive to changes in visual drive. In summary, our findings indicate that inhibitory and excitatory forms of plasticity are not independent events, but interact to shape cortical circuit connectivity and function in an experience-dependent fashion.

Plasticity of inhibitory synapses

Inhibitory synapses have been proposed as regulators of neuronal excitability (Carvalho and Buonomano, 2009) and mediators of experience-dependent refinement in local microcircuits (Maffei et al., 2006). The broad connectivity and powerful inhibition of FS in particular is thought to be highly effective in controlling the state of excitability of cortical neurons (Cardin et al., 2009). Such widespread connectivity has led to questioning FS involvement in fine scale regulation of cortical circuit connectivity (Smith and Bear, 2010). Our data demonstrate that FS can exert their inhibitory action in a connection-specific fashion by selectively inducing plasticity onto pyramidal neurons active within a well-identified range.

LTPi engages PT-sensitive Gi/o proteins activated by $GABA_B$ receptors located on the postsynaptic neurons. Whereas in the hippocampus activation of postsynaptic $GABA_B$ receptors requires GABA spillover from several inhibitory neurons (Scanziani, 2000), in L4 of V1 bursting of a single FS activates detectable $GABA_B$-IPSCs in pyramidal neurons. To induce LTPi, however, FS bursting was not sufficient. The postsynaptic neuron needed to be active during FS bursting. The requirement for postsynaptic depolarization initially led us to consider the involvement of calcium signaling through voltage gated channels in LTPi (Yoshimura et al., 2008). Our data indicate that LTPi is calcium independent. The depolarization may contribute to facilitating $GABA_B$- outward potassium currents, potassium inflow through voltage-gated channels, and/or chloride inflow to reduce excitability.

In addition to being calcium-independent, LTPi presented several differences from other forms of inhibitory synaptic plasticity; it is not expressed through changes in chloride reversal potential (Woodin et al., 2003) and does not require coactivation of glutamatergic receptors (Nugent and Kauer, 2008). Our previous work suggested that LTPi is expressed postsynaptically (Maffei et al., 2006). The data shown here support that interpretation and demonstrate that LTPi requires $GABA_B$ signaling, but does not rely on protein phosphatases. $GABA_B$–Gi/o signaling interferes with adenylcyclase (Duman and Enna, 1987) and can affect posttranslational modification of membrane receptors (Lüscher et al., 2011). Similar mechanisms may also contribute to LTPi.

Crosstalk of inhibitory and excitatory forms of plasticity

LTPi may reduce neuronal circuit excitability by impairing the ability of pyramidal neurons to generate action potentials (Saraga et al., 2008) and by affecting the capacity for plasticity at glutamatergic inputs. This effect could explain how inhibitory plastic-

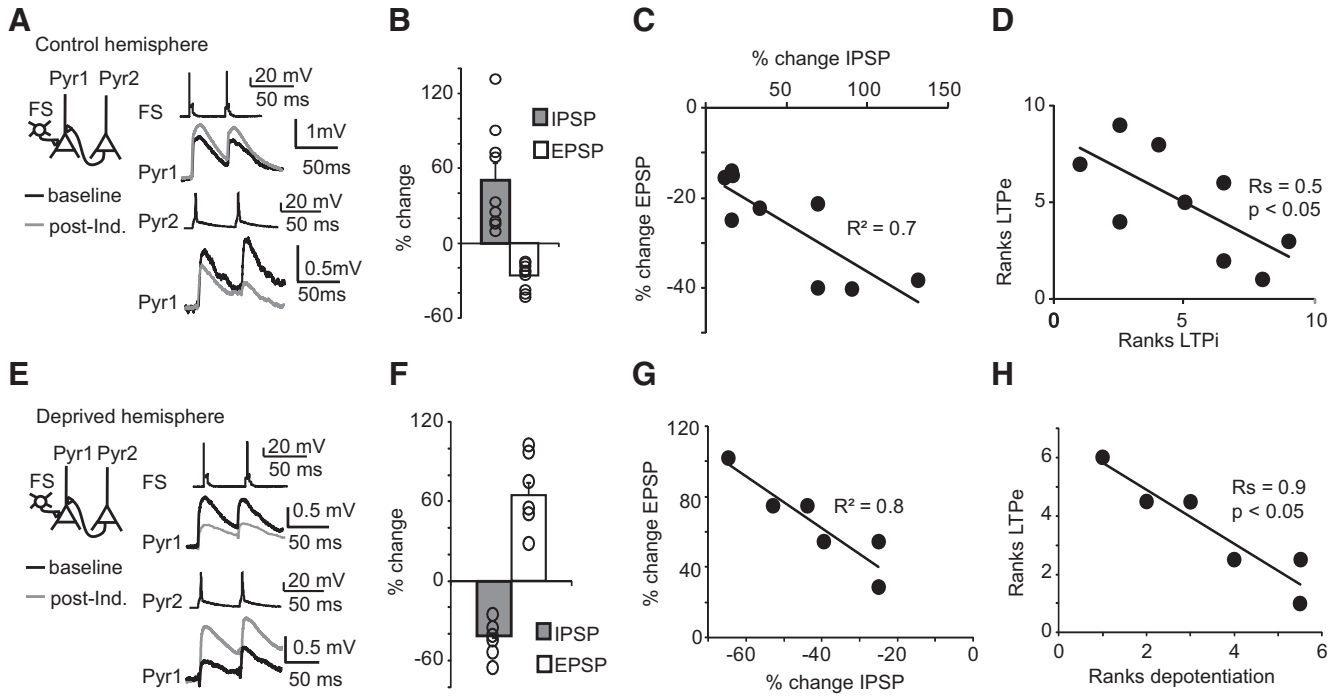

Figure 10. Experience-dependent modulation of the crosstalk between LTPi and LTPe. ***A***, Left, Diagram of recording configuration. Right, Sample traces of IPSP (top) and EPSP (bottom) before (black) and after (gray) coinduction of LTPi and LTPe in the control hemisphere of visually deprived rats. ***B***, Bar plot of percentage changes in IPSP (gray) and EPSP (white) amplitudes following coinduction. Open circles indicate single triplets. ***C***, Plot of LTPe versus LTPi magnitude. ***D***, Rank order correlation analysis of changes in IPSP and EPSP induced by coinduction. ***E***, Left, Diagram of recording configuration. Right, Sample traces of IPSP (top) and EPSP (bottom) before (black) and after (gray) coinduction of LTPi and LTPe in the deprived hemisphere. Note that IPSPs are depotentiated. ***F***, Bar plot of percentage changes in IPSP (gray) and EPSP (white) amplitudes following coinduction. Open circles indicate single triplets. ***G***, Plot of percentage change of EPSPs versus percentage changes of IPSPs in the deprived hemisphere. ***H***, Rank order correlation analysis of changes in EPSP and IPSP induced by coinduction. Data are mean ± SE. *P* values for Spearman rank order correlations are reported.

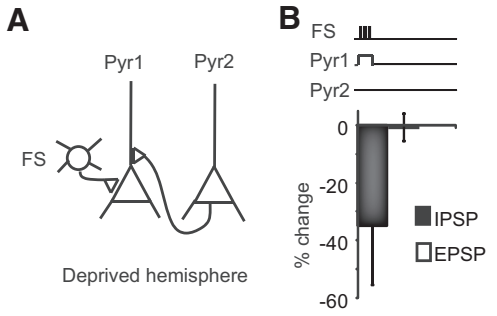

Figure 11. Induction of LTDi in the deprived hemisphere does not affect baseline EPSP amplitude. ***A***, Diagram of recording configuration. ***B***, Top, Induction paradigm during triplet recordings. Note that only the paradigm for LTPi was applied. Bottom, Bar plot of population changes in IPSP (black) and EPSP (white) amplitudes. Error bars represent SE ($n = 4$ triplets).

ity affects cortical gain in addition to neuronal input/output function (Carvalho and Buonomano, 2009). Activation of $GABA_B$–Gi/o during LTPi can interfere with LTPe through a number of signaling pathways. Gi/o signaling prevents opening of VGCC (Pérez-Garci et al., 2013) and opens potassium conductances (Chen and Johnston, 2005) that can hyperpolarize postsynaptic neurons (Lüscher and Slesinger, 2010). Affecting either of these mechanisms (or both) likely prevent increases in intracellular calcium that are critical for LTPe. We did not observe changes in resting membrane potential compatible with direct hyperpolarization of pyramidal neurons. However, blockade of L-type VGCC impaired LTPe and favored LTDe. In the cerebellum postsynaptic $GABA_B$, activation can enhance LTD at glutamatergic synapses (Kamikubo et al., 2007) via $GABA_B$-dependent

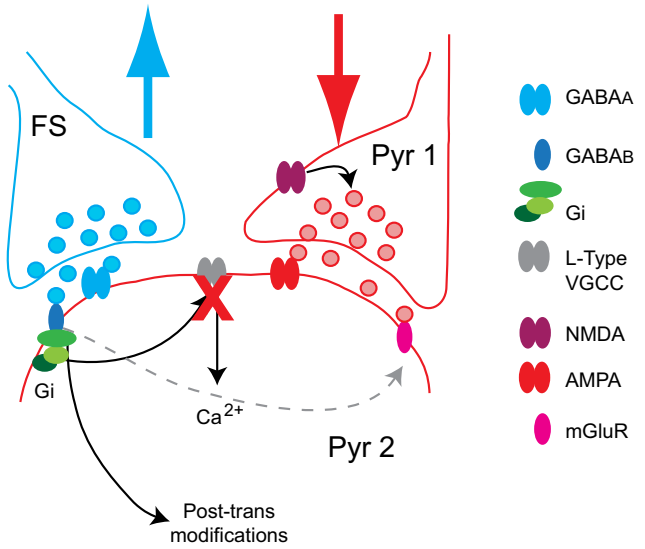

Figure 12. Summary diagram of the mechanisms of crosstalk between LTPi and LTPe. Model for crosstalk: GABA release from FS activates both $GABA_A$ and $GABA_B$ receptors on the postsynaptic pyramidal neuron. This leads to LTPi, a $GABA_B$–Gi/o-dependent potentiation of $GABA_A$-mediated IPSPs, onto Pyr2. In addition, it leads to a change in capacity for plasticity at the converging recurrent glutamatergic input from Pyr1 onto Pyr2. The mechanisms involved in changing the capacity for plasticity of the Pyr1–Pyr2 connection rely on Gi/o-dependent reduction in calcium inflow through L-type VGCC. Regulation of intracellular calcium levels (red X) could also be affected by activation of mGluR. In addition, coactivation of Group I mGluR contributes LTDe induction. Based on recent findings possible direct crosstalk between Gi/o and Group I mGluRs could be involved (dotted gray arrow).

activation of mGluRs (Rives et al., 2009). In L4 of V1, bursting of a presynaptic pyramidal neuron, whereas pharmacologically activating group I mGluRs, induces LTDe. The combination of Group I mGluR activation, $GABA_B$–Gi/o signaling and L-type VGCC blockade could explain both impairment of LTPe and induction of LTDe at excitatory inputs onto pyramidal neurons receiving potentiated inhibition.

Recurrent excitatory and inhibitory inputs in L4 of V1 are located in the perisomatic region (Bannister and Thomson, 2007). Although there is no direct report that these synapses are adjacent, recent studies in the hippocampus, in V1, and in other neocortical areas showed that GABAergic inputs can colocalize with glutamatergic synapses at spines (Chen et al., 2012; Chiu et al., 2013), likely favoring crosstalk of signaling mechanisms.

It was previously shown that glutamatergic transmission and plasticity coregulates inhibitory synapses (Nugent and Kauer, 2008). Our data demonstrate that the crosstalk can occur also in the opposite direction. In adult hippocampus, inhibitory synaptic plasticity depends on the level of expression of the chloride transporter KCC2 (Ormond and Woodin, 2011). Differently, LTPi does not affect chloride reversal potential (Maffei et al., 2006). Additional mechanisms of interactions proposed to date involve spillover of neurotransmitters onto nearby presynaptic terminals (Nugent et al., 2009), coactivation of $GABA_A$ and NMDA receptors (Komatsu and Iwakiri, 1993), coactivation of $GABA_A$ and 5HT-Gs protein signaling (Komatsu, 1996), or release of retrograde signals (Chevaleyre and Castillo, 2003). LTPi does not directly modulate EPSP amplitude or PPR, indicating that GABA spillover onto presynaptic glutamatergic terminals is unlikely to drive the crosstalk we report in V1. LTPi affects the capacity for plasticity at converging excitatory inputs that are coactivated during induction. Retrograde signaling cannot be fully excluded; however, to date there is no evidence suggesting presynaptic expression or release of retrograde signals during LTPi induction.

We did not explore the full extent of the time constrains for the crosstalk between LTPi and LTPe. However, we did test the effect of two intervals for coinduction (Fig. 5*C*). Both paradigms produced the same effect: successful LTPi and impaired LTPe. This indicates that the crosstalk between excitatory and inhibitory plasticity can occur at convergent inputs repetitively activated within a few seconds of one another. Such temporal interaction suggests that both transient and long-term Gi/o signaling mechanisms may be engaged. The involvement of short-term and long-term signaling pathways is further supported by LTPe dependence on L-type VGCC and intracellular calcium signaling. LTPi connection specificity, the relatively sparse recurrent connectivity of excitatory neurons (Bannister and Thomson, 2007; Wang et al., 2013), and the requirement for repetitive coactivation likely limit crosstalk to converging inputs driven by FS and pyramidal neurons with correlated activity. This constraint could allow for selectivity of the inputs affected by the crosstalk.

In the circuit used for this study, LTPi is induced by unilateral visual deprivation during the critical period for visual cortical plasticity (Maffei et al., 2006). Thus, LTPi has the potential to decrease excitability, and through the crosstalk of LTPi and excitatory plasticity, to selectively weaken excitatory inputs converging onto neurons driven by the deprived eye. Such interaction could explain the experience-dependent change from LTPe to LTDe at recurrent L4 excitatory inputs (Wang et al., 2012). Acute depotentiation of inhibition in the deprived hemisphere restores capacity for LTPe, consistent with a prominent role of inhibition in modulating the capacity for plasticity of V1 (Harauzov et al., 2010; Southwell et al., 2010). GABAergic inhibitory synapses are broadly distributed in the brain (Mohler et al., 1995) and inhibitory synapses contribute to experience dependent refinement (Maffei et al., 2006; Yazaki-Sugiyama et al., 2009; Richards et al., 2010; House et al., 2011; Chen et al., 2012), circuit excitability (Ben-Ari, 2006; Fritschy, 2008; Carvalho and Buonomano, 2009; Clarkson et al., 2010), learning (Kano, 1995; Fritschy and Brünig, 2003; Ruediger et al., 2011), and sensory processing (Cardin et al., 2009; Isaacson and Scanziani, 2011). The crosstalk of excitatory and inhibitory plasticity may thus be a general mechanism for fine-scale regulation of neural circuit connectivity and function.

References

Alitto HJ, Dan Y (2010) Function of inhibition in visual cortical processing. Curr Opin Neurobiol 20:340–346. CrossRef Medline

Bannister AP, Thomson AM (2007) Dynamic properties of excitatory synaptic connections involving layer 4 pyramidal cells in adult rat and cat neocortex. Cereb Cortex 17:2190–2203. CrossRef Medline

Belmeguenai A, Hansel C (2005) A role for protein phosphatases 1, 2A, and 2B in cerebellar long-term potentiation. J Neurosci 25:10768–10772. CrossRef Medline

Ben-Ari Y (2006) Seizures beget seizures: the quest for GABA as a key player. Crit Rev Neurobiol 18:135–144. CrossRef Medline

Cardin JA, Carlén M, Meletis K, Knoblich U, Zhang F, Deisseroth K, Tsai LH, Moore CI (2009) Driving fast-spiking cells induces gamma rhythm and controls sensory responses. Nature 459:663–667. CrossRef Medline

Carvalho TP, Buonomano DV (2009) Differential effects of excitatory and inhibitory plasticity on synaptically driven neuronal input-output functions. Neuron 61:774–785. CrossRef Medline

Chen JL, Villa KL, Cha JW, So PT, Kubota Y, Nedivi E (2012) Clustered dynamics of inhibitory synapses and dendritic spines in the adult neocortex. Neuron 74:361–373. CrossRef Medline

Chen X, Johnston D (2005) Constitutively active G-protein-gated inwardly rectifying K+ channels in dendrites of hippocampal CA1 pyramidal neurons. J Neurosci 25:3787–3792. CrossRef Medline

Chevaleyre V, Castillo PE (2003) Heterosynaptic LTD of hippocampal GABAergic synapses: a novel role of endocannabinoids in regulating excitability. Neuron 38:461–472. CrossRef Medline

Chiu CQ, Lur G, Morse TM, Carnevale NT, Ellis-Davies GC, Higley MJ (2013) Compartmentalization of GABAergic inhibition by dendritic spines. Science 340:759–762. CrossRef Medline

Chung HJ, Quian X, Ehlers M, Jan YN, Jan LY (2009) Neuronal activity regulates phosphorylation-dependent surface delivery of G-protein-activated inwardly rectifying potassium channels. Proc Natl Acad Sci U S A 106:629–634. CrossRef Medline

Clarkson AN, Huang BS, Macisaac SE, Mody I, Carmichael ST (2010) Reducing excessive GABA-mediated tonic inhibition promotes functional recovery after stroke. Nature 468:305–309. CrossRef Medline

Duman RS, Enna SJ (1987) Modulation of receptor-mediated cyclic AMP production in brain. Neuropharmacology 26:981–986. CrossRef Medline

Eto K, Ishibashi H, Yoshimura T, Watanabe M, Miyamoto A, Ikenaka K, Moorhouse AJ, Nabekura J (2012) Enhanced GABAergic activity in the mouse primary somatosensory cortex is insufficient to alleviate chronic pain behavior with reduced expression of neuronal potassium-chloride cotransporter. J Neurosci 32:16552–16559. CrossRef Medline

Fritschy JM (2008) Epilepsy, E/I balance and GABA(A) receptor plasticity. Front Mol Neurosci 1:5. CrossRef Medline

Fritschy JM, Brünig I (2003) Formation and plasticity of GABAergic synapses: physiological mechanisms and pathophysiological implications. Pharmacol Ther 98:299–323. CrossRef Medline

Galindo-Leon EE, Lin FG, Liu RC (2009) Inhibitory plasticity in a lateral band improves cortical detection of natural vocalizations. Neuron 62:705–716. CrossRef Medline

Gonchar Y, Pang L, Malitschek B, Bettler B, Burkhalter A (2001) Subcellular localization of GABA(B) receptor subunits in rat visual cortex. J Comp Neurol 431:182–197. CrossRef Medline

Haas JS, Nowotny T, Abarbanel HD (2006) Spike-timing-dependent plasticity of inhibitory synapses in the entorhinal cortex. J Neurophysiol 96:3305–3313. CrossRef Medline

Harauzov A, Spolidoro M, DiCristo G, De Pasquale R, Cancedda L, Pizzo-

russo T, Viegi A, Berardi N, Maffei L (2010) Reducing intracortical inhibition in the adult visual cortex promotes ocular dominance plasticity. J Neurosci 30:361–371. CrossRef Medline

Hayama T, Noguchi J, Watanabe S, Takahashi N, Hayashi-Takagi A, Ellis-Davies GC, Matsuzaki M, Kasai H (2013) GABA promotes the competitive selection of dendritic spines by controlling local Ca(2+) signaling. Nat Neurosci 16:1409–1416. CrossRef Medline

Heimel JA, van Versendaal D, Levelt CN (2011) The role of GABAergic inhibition in ocular dominance plasticity. Neural Plast 2011:391763. CrossRef Medline

Hensch TK, Fagiolini M (2005) Excitatory-inhibitory balance and critical period plasticity in developing visual cortex. Prog Brain Res 147:115–124. CrossRef Medline

Hirono M, Yoshioka T, Konishi S (2001) GABA(B) receptor activation enhances mGluR-mediated responses at cerebellar excitatory synapses. Nat Neurosci 4:1207–1216. CrossRef Medline

Holmgren CD, Zilberter Y (2001) Coincident spiking activity induces long-term changes in inhibition of neocortical pyramidal cells. J Neurosci 21: 8270–8277. Medline

House DR, Elstrott J, Koh E, Chung J, Feldman DE (2011) Parallel regulation of feedforward inhibition and excitation during whisker map plasticity. Neuron 72:819–831. CrossRef Medline

Isaacson JS, Scanziani M (2011) How inhibition shapes cortical activity. Neuron 72:231–243. CrossRef Medline

Kamikubo Y, Tabata T, Kakizawa S, Kawakami D, Watanabe M, Ogura A, Iino M, Kano M (2007) Postsynaptic GABAB receptor signalling enhances LTD in mouse cerebellar Purkinje cells. J Physiol 585:549–563. CrossRef Medline

Kano M (1995) Plasticity of inhibitory synapses in the brain: a possible memory mechanism that has been overlooked. Neurosci Res 21:177–182. CrossRef Medline

Komatsu Y (1996) GABAB receptors, monoamine receptors, and postsynaptic inositol trisphosphate-induced Ca2+ release are involved in the induction of long-term potentiation at visual cortical inhibitory synapses. J Neurosci 16:6342–6352. Medline

Komatsu Y, Iwakiri M (1993) Long-term modification of inhibitory synaptic transmission in developing visual cortex. Neuroreport 4:907–910. CrossRef Medline

Kurotani T, Yamada K, Yoshimura Y, Crair MC, Komatsu Y (2008) State-dependent bidirectional modification of somatic inhibition in neocortical pyramidal cells. Neuron 57:905–916. CrossRef Medline

Lüscher B, Fuchs T, Kilpatrick CL (2011) GABAA receptor trafficking-mediated plasticity of inhibitory synapses. Neuron 70:385–409. CrossRef Medline

Lüscher C, Slesinger PA (2010) Emerging roles for G-protein-gated inwardly rectifying potassium (GIRK) channels in health and disease. Nat Rev Neurosci 11:301–315. CrossRef Medline

Madhavan A, Bonci A, Whistler JL (2010) Opioid-induced GABA potentiation after chronic morphine attenuates the rewarding effects of opioids in the ventral tegmental area. J Neurosci 30:14029–14035. CrossRef Medline

Maffei A, Turrigiano GG (2008) Multiple modes of network homeostasis in visual cortical layer 2/3. J Neurosci 28:4377–4384. CrossRef Medline

Maffei A, Nelson SB, Turrigiano GG (2004) Selective reconfiguration of layer 4 visual cortical circuitry by visual deprivation. Nat Neurosci 7:1353–1359. CrossRef Medline

Maffei A, Nataraj K, Nelson SB, Turrigiano GG (2006) Potentiation of cortical inhibition by visual deprivation. Nature 443:81–84. CrossRef Medline

Maffei A, Lambo ME, Turrigiano GG (2010) Critical period for inhibitory plasticity in rodent binocular V1. J Neurosci 30:3304–3309. CrossRef Medline

Mansuy IM, Shenolikar S (2006) Protein serine/threonine phosphatases in neuronal plasticity and disorders of learning and memory. Trends Neurosci 29:679–686. CrossRef Medline

Mohler H, Knoflach F, Paysan J, Motejlek K, Benke D, Lüscher B, Fritschy JM (1995) Heterogeneity of GABAA-receptors: cell-specific expression, pharmacology, and regulation. Neurochem Res 20:631–636. CrossRef Medline

Nugent FS, Kauer JA (2008) LTP of GABAergic synapses in the ventral tegmental area and beyond. J Physiol 586:1487–1493. CrossRef Medline

Nugent FS, Penick EC, Kauer JA (2007) Opioids block long-term potentiation of inhibitory synapses. Nature 446:1086–1090. CrossRef Medline

Nugent FS, Niehaus JL, Kauer JA (2009) PKG and PKA signaling in LTP at GABAergic synapses. Neuropsychopharmacology 34:1829–1842. CrossRef Medline

Nusser Z, Hájos N, Somogyi P, Mody I (1998) Increased number of synaptic GABAA receptors underlies potentiation at hippocampal inhibitory synapses. Nature 395:172–177. CrossRef Medline

Ormond J, Woodin MA (2009) Disinhibition mediates a form of hippocampal long-term potentiation in area CA1. PLoS One 4:e7224. CrossRef Medline

Ormond J, Woodin MA (2011) Disinhibition-mediated LTP in the hippocampus is synapse specific. Front Cell Neurosci 5:17. CrossRef Medline

Pérez-Garci E, Larkum ME, Nevian T (2013) Inhibition of dendritic Ca2+ spikes by GABAB receptors in cortical pyramidal neurons is mediated by a direct Gi/o-β subunit interaction with Cav1 channels. J Physiol 591: 1599–1612. CrossRef Medline

Pettit DL, Augustine GJ (2000) Distribution of functional glutamate and GABA receptors on hippocampal pyramidal cells and interneurons. J Neurophysiol 84:28–38. Medline

Richards BA, Voss OP, Akerman CJ (2010) GABAergic circuits control stimulus-instructed receptive field development in the optic tectum. Nat Neurosci 13:1098–1106. CrossRef Medline

Rives ML, Vol C, Fukazawa Y, Tinel N, Trinquet E, Ayoub MA, Shigemoto R, Pin JP, Prézeau L (2009) Crosstalk between GABAB and mGlu1a receptors reveals new insight into GPCR signal integration. EMBO J 28:2195–2208. CrossRef Medline

Ruediger S, Vittori C, Bednarek E, Genoud C, Strata P, Sacchetti B, Caroni P (2011) Learning-related feedforward inhibitory connectivity growth required for memory precision. Nature 473:514–518. CrossRef Medline

Saraga F, Balena T, Wolansky T, Dickson CT, Woodin MA (2008) Inhibitory synaptic plasticity regulates pyramidal neuron spiking in the rodent hippocampus. Neuroscience 155:64–75. CrossRef Medline

Scanziani M (2000) GABA spillover activates postsynaptic GABA(B) receptors to control rhythmic hippocampal activity. Neuron 25:673–681. CrossRef Medline

Smith GB, Bear MF (2010) Bidirectional ocular dominance plasticity of inhibitory networks: recent advances and unresolved questions. Front Cell Neurosci 4:21. CrossRef Medline

Southwell DG, Froemke RC, Alvarez-Buylla A, Stryker MP, Gandhi SP (2010) Cortical plasticity induced by inhibitory neuron transplantation. Science 327:1145–1148. CrossRef Medline

Sugiyama Y, Kawaguchi SY, Hirano T (2008) mGluR1-mediated facilitation of long-term potentiation at inhibitory synapses on a cerebellar Purkinje neuron. Eur J Neurosci 27:884–896. CrossRef Medline

Wang L, Fontanini A, Maffei A (2012) Experience-dependent switch in sign and mechanisms for plasticity in layer 4 of primary visual cortex. J Neurosci 32:10562–10573. CrossRef Medline

Wang L, Kloc M, Gu Y, Ge S, Maffei A (2013) Layer-specific experience-dependent rewiring of thalamocortical circuits. J Neurosci 33:4181–4191. CrossRef Medline

Woodin MA, Ganguly K, Poo MM (2003) Coincident presynaptic and postsynaptic activity modifies GABAergic synapses by postsynaptic changes in Cl− transporter activity. Neuron 39:807–820. CrossRef Medline

Yazaki-Sugiyama Y, Kang S, Câteau H, Fukai T, Hensch TK (2009) Bidirectional plasticity in fast-spiking GABA circuits by visual experience. Nature 462:218–221. CrossRef Medline

Yoshimura Y, Inaba M, Yamada K, Kurotani T, Begum T, Reza F, Maruyama T, Komatsu Y (2008) Involvement of T-type Ca2+ channels in the potentiation of synaptic and visual responses during the critical period in rat visual cortex. Eur J Neurosci 28:730–743. CrossRef Medline